Novel Device and Strategy for Growing Large, High-Quality Protein Crystals by Controlling Crystallization Conditions

Naoki Tanigawa [1], Sachiko Takahashi [2], Bin Yan [2], Masayuki Kamo [3], Naoki Furubayashi [3], Koji Kubota [1], Koji Inaka [3] and Hiroaki Tanaka [2,*]

[1] Chiyoda Corporation, 3-13 Moriya-cho, Kanagawa-ku, Kanagawa, Yokohama 221-0022, Japan; tanigawa.naoki@chiyodacorp.com (N.T.); koji.kubota.zj@alum.riken.jp (K.K.)
[2] Confocal Science Incorporated, 5-14-15 Fukasawa, Setagaya-ku, Tokyo 158-0081, Japan; takahashis@confsci.co.jp (S.T.); yanb@confsci.co.jp (B.Y.)
[3] Maruwa Foods and Biosciences Incorporated, 170-1 Tsutsui-cho, Yamatokoriyama, Nara 639-1123, Japan; masayuki_kamo@maruwafoods.jp (M.K.); furubayashi@maruwafoods.jp (N.F.); inaka@maruwafoods.jp (K.I.)
* Correspondence: tanakah@confsci.co.jp; Tel.: +81-3-3864-6606

Abstract: Neutron diffraction experiments are informative for determining the locations of hydrogen atoms in protein molecules; however, much larger crystals are needed than those required for X-ray diffraction. Thus, additional techniques are required to grow larger crystals. Here, a unique crystallization device and strategy for growing large protein crystals are introduced. The device uses two micropumps to control crystal growth by altering the precipitant concentration and regulating the pinpoint injection of dry air flow to the crystallization cell. Furthermore, the crystal growth can be observed in real time. Preliminary microbatch crystallization experiments at various concentration ranges of polyethylene glycol (PEG) 4000 and sodium chloride were first performed to elucidate optimized crystallization conditions. Based on these results, a device to precisely control the sodium chloride and PEG concentrations and the supply of dry air to the crystallization cell was used, and 1.8 mm lysozyme and 1.5 mm alpha-amylase crystals with good reproducibility were obtained. X-ray data sets of both crystals were collected at room temperature at BL2S1 of the Aichi Synchrotron Radiation Center and confirmed that these crystals were of high quality. Therefore, this crystallization device and strategy were effective for growing large, high-quality protein crystals.

Keywords: neutron diffraction; large crystal; reservoir control; real-time observation

1. Introduction

While X-ray diffraction only reveals the electron density, neutron diffraction can provide complementary data to X-ray diffraction regarding the position of hydrogen atoms and the protonation status to provide a complete biological structure [1]. Therefore, neutron protein crystallography has received considerable interest to investigate the enzymatic reaction mechanism. Neutron protein crystallography has recently improved, both in terms of hardware and software: new and improved beamlines, software, and novel techniques for growing larger crystals [2–5]. However, only 0.1% of the structural data deposited in the Research Collaboratory for Structural Bioinformatics Protein Data Bank (PDB) used neutron diffraction to determine the macromolecule structure (as of September 2021). This is mainly because neutron diffraction requires much larger cubic crystals (~1 mm^3) compared with those needed for X-ray diffraction.

To grow such large crystals, the control of the nucleation to decrease its probability is one of the necessary processes. The nucleation process has been studied extensively [6], but the difficulties to grow such crystals have not been resolved. Another method is to use a counter-diffusion method with a large bore capillary and to apply the optimum pH to enhance the Ostwald ripening [7]. Ostwald ripening [8] is a process in which small crystals are absorbed into a larger, more stable crystal. Because the overall interfacial energy is

dependent on ionizable sites on the crystal surface, the pH of the growth solution should be a value close to the pKa of the ionizable groups on the protein molecule to enhance the ripening [7]. However, to grow one large crystal, additional investigation is required to obtain a numerical method that can elucidate quantitative experimental conditions. Nakamura et al. [9] recently introduced a method for estimating the optimal experimental conditions for growing single large crystals using defined volumes of a sample solution. The method combines preliminary microbatch experiments with a numerical model, resulting in more efficient and rational crystallization experiments. However, this method still required a prohibitively long time for growing large single crystals.

A semiautomated crystallization apparatus was previously designed to rationally grow large protein crystals using a temperature-controlled dialysis method [10,11]. While the automatic control of crystallization and thermal conditions is beneficial, thermal control may not be preferable for the crystallization of temperature-sensitive crystals.

Niimura & Podjarny [3] introduced a dialysis method to determine the crystallization phase diagram using a device in which pumps were used to control the protein and precipitant concentrations.

Here, we have developed a novel and unique device and protocol for growing large crystals. This device enables the growth of large crystals by controlling the crystallization conditions in real time with observation. In this device, two micropumps are connected to the crystallization cell. One micropump controls the composition of the reservoir solution in the reservoir container with a microdialysis probe. The other micropump controls the local concentration of protein in the crystallization cell by flowing dry air through the other probe to stimulate nucleation. By activating and inactivating these micropumps, the crystallization conditions and nucleation stimulation can be controlled while observing the state of crystal growth in real time through a microscope focused on the crystallization cell.

Before attempting protein crystallization using this device, preliminary microbatch crystallization experiments were conducted. These used a relatively small amount of protein sample to identify the optimized crystallization solution by defining the sodium chloride and PEG 4000 concentrations where the nucleation probability was low and single crystals would grow [12].

According to the preliminary batch method results, a favorable crystallization condition that allowed a small number of crystals to grow as single crystals was first applied in this device. The crystallization condition was then altered using the micropumps to grow larger crystals.

In this contribution, we introduce the details of this device and strategy. We also present the results of using this device to grow large crystals of lysozyme and alpha-amylase as example proteins.

2. Crystallization Device

2.1. Description of the Crystallization Device

The designed crystallization device is shown in Figure 1. A crystallization cell with an inner diameter of 2 mm and a length of 18 mm (MB2004-CRT804G-2 or MB2004-CRT803Q2-2; Confocal Science Inc., Tokyo, Japan) is connected to a reservoir container at the end of the cell via a dialysis membrane probe (reservoir probe) (6000 Da molecular weight cutoff; CMA11; CMA Microdialysis, Kista, Sweden). The reservoir solution is supplied to the crystallization cell through this probe, which is regulated by a micropump (RP-QII1.5S-P90Z-DC3V; Aquatech, Osaka, Japan). Protein molecules greater than 6000 Da are retained within the crystallization cell. By infusing and draining the reservoir solution through the reservoir probe, the crystallization condition can be controlled. A relief valve between the reservoir probe and the reservoir container prevents the reservoir probe from being overpressurized. The optimum flow rate was 100 to 240 μL/min. The other end of the crystallization cell is connected to a desiccator that provides dry air via an RTV (room-temperature-vulcanizing) silicone-coated dialysis membrane probe (dry air probe) and is controlled by a micropump of the same type as for the reservoir solution. The

membrane coating is necessary to prevent water permeation, as well as salt precipitation in the probe. By managing the dry and moist air supplied and exhausted through the dry air probe, the protein concentration in the vicinity of this probe is increased, which stimulates crystal nucleation. These pumps are activated and inactivated as needed while observing crystal growth in the crystallization cell under a microscope.
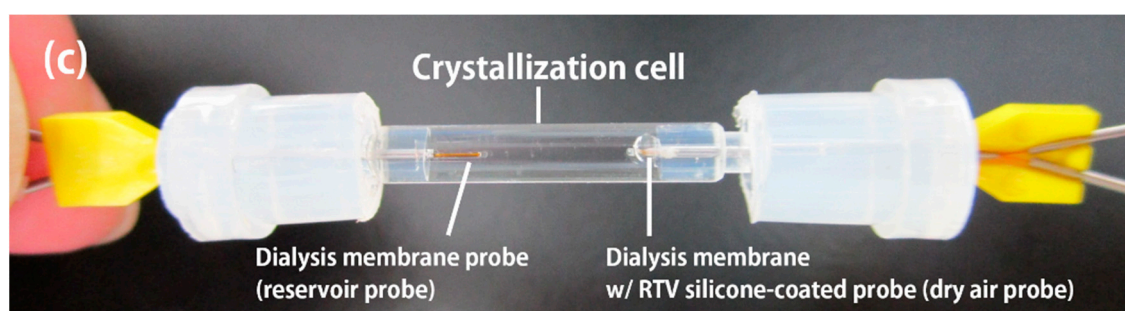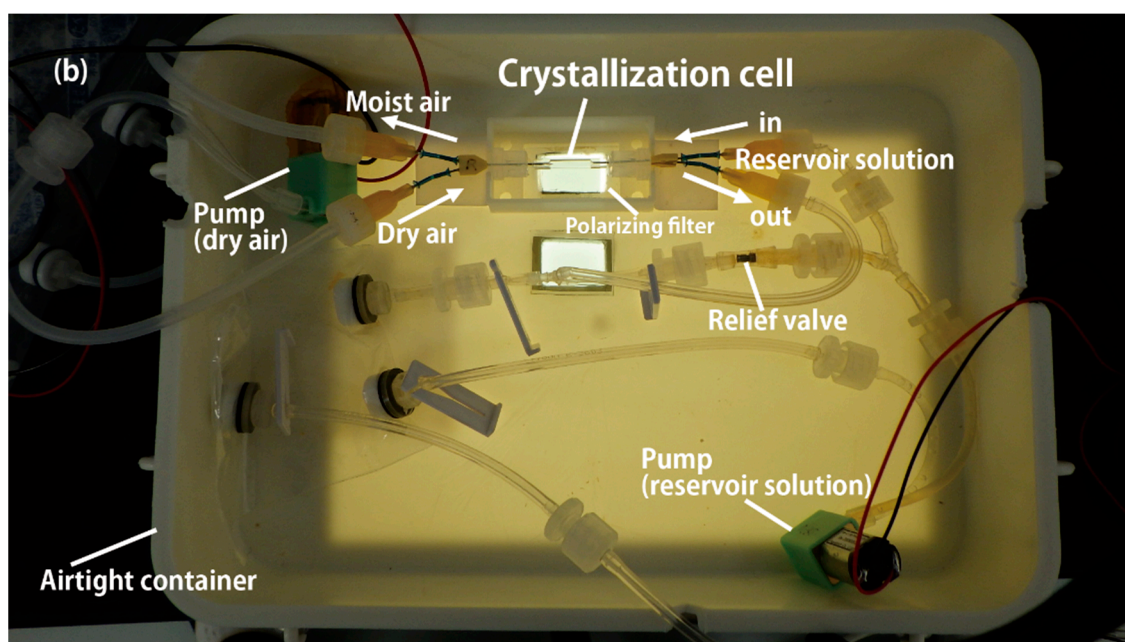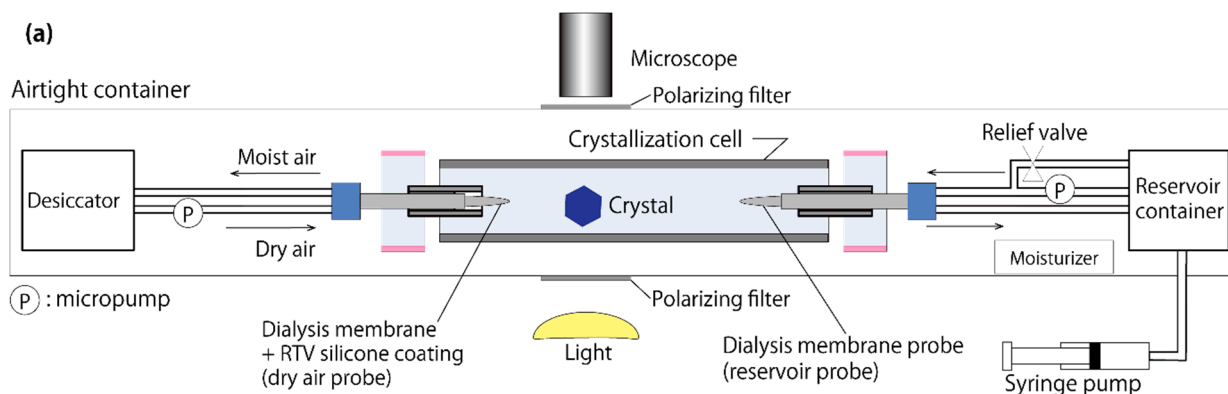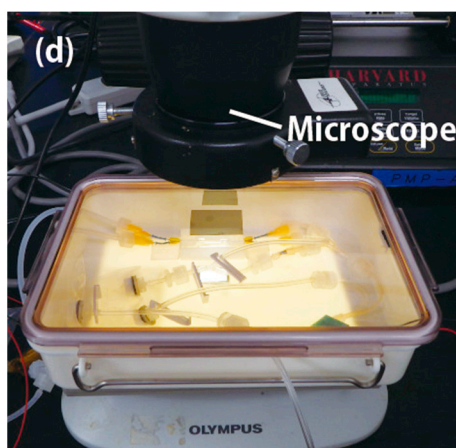

Figure 1. *Cont.*

Figure 1. The crystallization device. (**a**) A conceptual diagram of the crystallization device; (**b**) overview of the device; (**c**) crystallization cell; (**d**) real-time observation system.

2.2. Verification of Reservoir Probe Performance

To verify the performance of the reservoir probe, a refractometer (RA-520N; Kyoto Electronics Manufacturing Co., Ltd., Kyoto, Japan) was used to measure the increase in crystallization cell concentration of polyethylene glycol (PEG) 4000 and ammonium sulfate (AS) 24 h after filling the reservoir container with 10% (*w/v*) PEG 4000 and 20% (*w/v*) AS, respectively. We chose these reagents because they are commonly used in protein crystallization experiments.

The initial concentration increase via the reservoir probe was 1.35% (*w/v*) PEG 4000/day and 16.3% AS/day. The initial reservoir concentration was 10% (*w/v*) PEG 4000 and 20% AS. The lysozyme protein molecules were confirmed not to permeate.

Using these flow rates, we calculated the time needed to increase the concentrations of PEG 4000 and AS in the crystallization cell to half of the reservoir solution, which were 301 h for PEG 4000 and 9.8 h for AS. Using these values, we estimated the concentration change of PEG 4000 and sodium chloride in the crystallization cell, as shown in Sections 3.1.2 and 3.2.2.

2.3. Verification of Dry Air Probe Performance

To verify the crystallization performance of the dry air probe, we investigated the effect of the presence or absence of dry air on lysozyme crystallization. Lysozyme (100 mg/mL) and 5% (*w/v*) PEG 4000 in 50 mM sodium acetate buffer pH 4.5 were loaded into the crystallization cell, and 5% (*w/v*) PEG 4000 and 300 mM sodium chloride in 50 mM sodium acetate buffer pH 4.5 was loaded into the reservoir container. The sodium chloride (300 mM) concentration is at the boundary of lysozyme crystallization.

When the reservoir solution was supplied to the crystallization cell, crystals appeared only if dry air was also supplied, although the amount of the solution in the crystallization cell was not significantly decreased (data not shown). This showed that supplying dry air through the probe could effectively generate crystals. This is thought to have occurred by stimulating crystal nucleation by increasing the local concentration of the solution around the probe where the crystallization condition was at the boundary of crystal formation.

3. Large Crystal Growth in the Device

3.1. Lysozyme Crystallization

3.1.1. Preliminary Crystallization by the Microbatch Method to Develop a Crystallization Strategy

Preliminary microbatch crystallization was performed at 20 degrees Celsius as previously described [9] in the concentration ranges of 0 to 25% (*w/v*) PEG 4000 (95904-250G-F; Millipore Sigma, MA, USA) and 100 to 1000 mM sodium chloride (191-01665; FUJIFILM

Wako Pure Chemical Corporation, Tokyo, Japan). The lysozyme concentration was at 25 mg/mL (MB-P-AA001; Confocal Science Inc.). All solutions were dissolved in 50 mM sodium acetate buffer pH 4.5 (sodium acetate trihydrate (195-05085; FUJIFILM Wako Pure Chemical Corporation) and acetic acid (A6283-100ML; Millipore Sigma)). Each crystallization experiment was carried out in duplicate. After seven days, the number of single and clustered crystals was counted by visual inspection, and the number of crystals in a unit volume (1 μL) and the ratio of single crystals to all crystals in each crystallization condition were calculated (Table 1). In solutions with lower PEG 4000 concentrations (0% (*w/v*) and 5% (*w/v*)), single crystals tended to grow more than clustered crystals. In solutions with higher PEG 4000 concentrations (10% (*w/v*) and 15% (*w/v*)), the number of crystals increased. At higher PEG 4000 concentrations (20% (*w/v*) and 25% (*w/v*)), the number of crystals decreased, and there were more clustered crystals than single crystals. The nucleation probability tended to be higher at medium sodium chloride concentrations. These results are qualitatively consistent with nucleation theory [13–15].

Table 1. Number of crystals in unit volume and the ratio of single crystals of lysozyme grown by microbatch crystallization in sodium chloride and PEG 4000. The table shows the number of crystals per unit volume (1 μL) (top number) and the ratio of single crystals to all crystals (bottom number) seven days after crystallization setup.

		Sodium Chloride (mM)									
		100	200	300	400	500	600	700	800	900	1000
PEG 4000 (%(*w/v*))	25	0	6	13	9	6	11	6	8	7	4
		-	0.38	0.20	0.20	0.22	0.36	0.43	0.22	0.10	0.17
	20	4	ND	10	8	8	11	6	15	17	9
		0.00	ND	0.60	0.60	0.20	0.20	0.40	0.33	0.20	0.25
	15	21	ND	25	41	44	64	171	86	ND	51
		0.25	ND	0.27	0.33	0.33	0.41	0.20	0.20	ND	0.00
	10	13	24	13	42	118	ND	66	68	40	42
		0.25	0.80	0.67	0.50	0.79	ND	0.57	0.59	0.26	0.23
	5	0	3	0	ND	13	8	8	13	37	ND
		-	1.00	-	ND	0.60	0.50	0.75	0.33	0.50	ND
	0	0	0	0	33	13	19	ND	17	20	23
		-	-	-	0.88	0.83	1.00	ND	0.83	0.71	0.67

ND: No data. The color depth of the cell corresponds to the single crystal ratio (red) and the number of crystals (green).

To verify the quality of the lysozyme crystals grown in the preliminary microbatch method, X-ray diffraction data were collected on the i04-1 beamline at the Diamond Light Source, Oxford, UK [16]. Table 2 shows that all crystals gave good diffraction data in terms of maximum resolution and mosaicity. The data were processed using the autoProc pipeline [17]. The best crystals grew in 25% (*w/v*) PEG 4000 and 1 M sodium chloride, which may be due to PEG-induced depletion attraction [18].

Taken together, these results could lead to a strategy for growing large crystals by changing the crystallization conditions during crystal growth as follows: start the crystallization experiment with low concentrations of sodium chloride and PEG 4000 to initiate the nucleation of a small number of good-shaped crystal (not clustered). Next, increase the concentration of sodium chloride while observing the crystals, and then increase the concentration of PEG 4000 to further grow the crystals larger.

Table 2. Maximum resolution of lysozyme crystals grown in various concentrations of sodium chloride and PEG 4000 by the microbatch method. The X-ray diffraction data (maximum resolution (Å) and mosaicity (°)) were obtained at the Diamond Light Source i04-1. The data were processed using the autoProc pipeline. Most of the experiments were performed at least in duplicate, except for the single case shown without the standard deviation.

| | | Sodium Chloride (mM) | | | | | |
| | | 400 | | 700 | | 1000 | |
		Maximum Resolution (Å)	Mosaicity (°)	Maximum Resolution (Å)	Mosaicity (°)	Maximum Resolution (Å)	Mosaicity (°)
PEG 4000 (% (*w/v*))	25	1.06 ± 0.03	0.12 ± 0.03	1.03 ± 0.02	0.12 ± 0.03	1.01 ± 0.01	0.09 ± 0.00
	20	1.13 ± 0.05	0.14 ± 0.03	1.10	0.09	1.11 ± 0.00	0.12 ± 0.01
	10	1.08 ± 0.02	0.11 ± 0.01	1.19 ± 0.06	0.15 ± 0.01	1.10 ± 0.02	0.11 ± 0.01
	5	1.11 ± 0.01	0.11 ± 0.01	1.07 ± 0.01	0.12 ± 0.02	1.10 ± 0.01	0.10 ± 0.01
	0	1.12 ± 0.06	0.11 ± 0.02	1.14	0.15	1.08 ± 0.02	0.11 ± 0.02

To examine the solubility of lysozyme under each crystallization condition, after finishing crystal growth, the lysozyme concentration in the crystallization cell was measured by the Bradford assay [19] using a spectrometer (SSEC2000 UV/VIS, BAS, Tokyo, Japan) at 595 nm (Table 3). Increasing concentrations of PEG 4000 and sodium chloride reduced the solubility of lysozyme. This suggested that when a crystal is growing in a certain crystallization condition, the crystal might grow larger if the crystallization condition is changed to a higher concentration of PEG 4000 and sodium chloride in which the solubility of lysozyme is lower.

Table 3. Solubility of lysozyme in various concentrations of sodium chloride and PEG 4000. The solubility of lysozyme (mg/mL) was obtained by measuring the residual lysozyme concentration in the crystallization cell after crystal growth was completed.

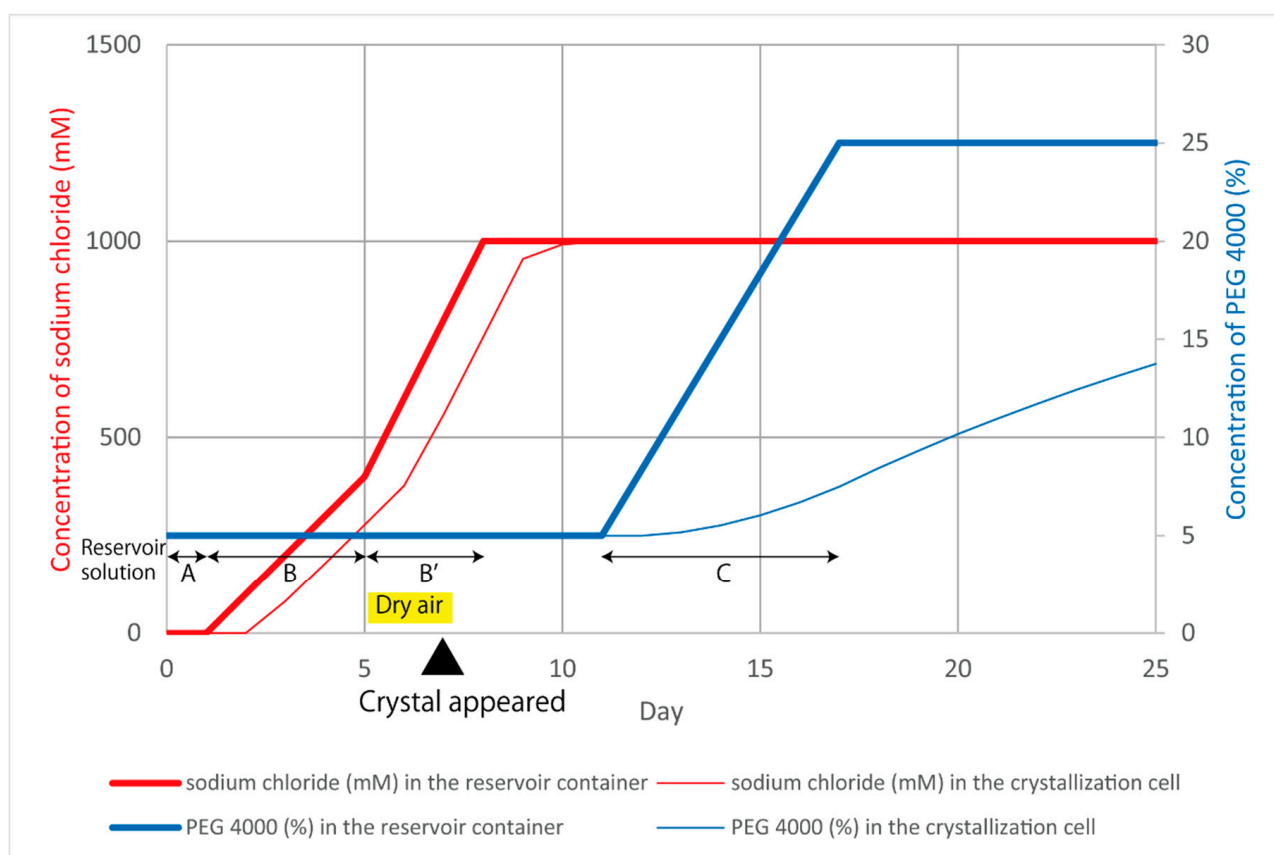| | | Sodium Chloride (mM) | | | | | | | | | |
		100	200	300	400	500	600	700	800	900	1000
PEG 4000 (%(*w/v*))	25	-	3.6	-	2.2	-	-	1.8	-	-	-
	20	8.6	5.7	3.8	2.9	2.3	2.7	4.8	4.1	3.3	2.8
	15	14.2	6.2	5.7	3.0	2.6	2.0	2.5	2.0	1.7	1.9
	10	17.1	6.2	5.6	5.0	4.4	4.0	3.1	3.5	3.5	3.4
	5	27.4	5.5	5.5	5.2	5.5	4.7	3.4	2.7	1.8	1.6
	0	-	14.6	12.4	6.9	4.9	3.7	3.7	2.6	3.6	2.5

The color depth of the cell corresponds to the solubility of lysozyme.

### 3.1.2. Lysozyme Crystallization Using the Device to Grow Large Crystals

Based on the results of microbatch crystallization, we developed a strategy to grow larger crystals. By shifting the crystallization conditions, it was predicted that it is possible to first produce a small number of well-shaped crystals and then grow them to a large size.

Crystallization was performed at 20 degrees Celsius in the device following the procedure in Figure 2. The lysozyme solution in the crystallization cell was 30 μL of 50 mg/mL lysozyme and 5% (*w/v*) PEG 4000. Initially, 5 mL of 5% (*w/v*) PEG 4000 in 50 mM sodium acetate buffer pH 4.5 (Reservoir A) was filled in the reservoir container and flowed at 100 μL/min into the crystallization cell to confirm the absence of crystallization. On Day 1, 5% (*w/v*) PEG 4000 and 2 M sodium chloride in 50 mM sodium acetate buffer pH 4.5 (Reservoir B) was flowed into the reservoir container at a flow rate of 0.2 μL/min to increase the sodium chloride concentration. Because no crystals were observed by Day 5, the flow rate was changed to 0.4 μL/min to gradually increase the concentration of sodium

chloride while observing the crystallization. At the same time, to stimulate nucleation, dry air was fed through the dry air probe at a flow rate of 0.5 mL/min until the first crystal was observed. On Day 7, before the concentration of sodium chloride in the reservoir container reached 1 M, a few crystals of approximately 1.2 mm length (long side) were observed, and the dry air supply was stopped. When the concentration of sodium chloride reached 1 M in the reservoir container, the supply of the reservoir solution was stopped, and these crystals continued to grow for a few more days. On Day 11, the crystals were determined to be sufficiently large; hence, 50% (*w/v*) PEG 4000 and 1 M sodium chloride in 50 mM sodium acetate buffer pH 4.5 (Reservoir C) was flowed to the reservoir container at a flow rate of 2 μL/min to increase the concentration of PEG 4000. When the concentration of PEG 4000 in the reservoir container reached 25% (*w/v*), the size of the crystal was approximately 1.8 mm (Figure 3).

Figure 2. Controlling lysozyme crystallization conditions by changing the reservoir solution. The concentrations of sodium chloride and PEG 4000 in the reservoir container are shown as thick red and blue lines, respectively. The concentrations of those in the crystallization cell are estimated numerically and shown as thin red and blue lines, respectively. The reservoir solution flowing to the reservoir container was changed as indicated by the black double arrows: A, 5% (*w/v*) PEG 4000 at a flow rate of 100 μL/min; B, 5% (*w/v*) PEG 4000 + 2 M sodium chloride at a flow rate of 0.2 μL/min; B', 5% (*w/v*) PEG 4000 + 2 M sodium chloride at a flow rate of 0.4 μL/min; C, 50% (*w/v*) PEG 4000 + 1 M sodium chloride at a flow rate of 2 μL/min. All solutions were dissolved in 50 mM sodium acetate buffer pH 4.5. Dry air was supplied at a flow rate of 0.5 mL/min from the beginning of B' until the first crystal was observed.
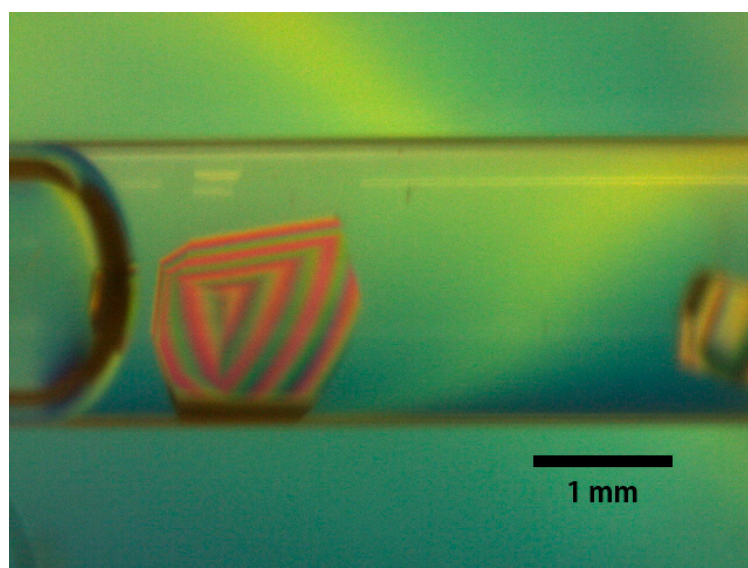
Figure 3. Lysozyme crystals grown in the crystallization cell. The crystal was approximately 1.8 mm on its longest side.

Thus, the crystallization strategy based on preliminary experiments worked well and as planned. Nucleation started at low concentrations of sodium chloride and PEG 4000. Single crystals grew as the concentration of sodium chloride increased while observing the crystals, and then the increased concentration of PEG 4000 further enabled crystal growth. When the first crystals were observed, the sodium chloride and PEG 4000 concentrations in the crystallization cell were estimated to be approximately 500 mM and 5% (w/v), respectively (Figure 2), which is consistent with the preliminary crystallization conditions in Table 1.

To verify the quality of the lysozyme crystals, they were subjected to X-ray diffraction at room temperature by applying a wavelength of 1.12 Å at the BL2S1 beamline at AichiSR, Japan, with an ADSC 315r detector system [20]. The crystallization cell was cut by a file to remove the mother liquor around the crystals. The end of the crystallization cell was sealed with wax (HR4-328, Hampton Research, CA, USA) to prevent solvent evaporation and then mounted to the goniometer head. The data were collected at 293 K. A total of 360 frames were collected using a crystal-to-detector distance of 146.1 mm, with a 5-s exposure time and a 0.5° oscillation angle. The diffraction images were integrated and refined using iMosflm and Aimless in the CCP4 suite [21,22].

The data collection and processing statistics are shown in Table 4. The maximum resolution was 1.39 Å with low mosaicity (0.07°). The crystals were not damaged, even after collecting two data sets with the same crystal. Compared to the X-ray diffraction data of lysozyme crystals grown in a similar configuration without pumps, the maximum resolution of the lysozyme crystals grown in this device was similar, but its mosaicity was very low (0.39° for the crystal without real-time observation). We concluded that the crystallization device and strategy were effective not only for growing large crystals but also high-quality crystals of lysozyme.

Table 4. Data collection and processing of lysozyme crystals.

Diffraction Source	BL2S1, AichiSR
Wavelength (Å)	1.12
Temperature (K)	293
Detector	ADSC 315r
Crystal-detector distance (mm)	146.1
Rotation range per image (°)	0.5
Total rotation range (°)	180
Exposure time per image (s)	5
Space group	$P4_32_12$
a, b, c (Å)	79.1, 79.1, 38.2
α, β, γ (°)	90, 90, 90
Mosaicity (°)	0.07
Resolution range (Å)	79.08–1.39 (1.41–1.39)
Total No. of reflections	343,623 (15,609)
No. of unique reflections	24,976 (1229)
Completeness (%)	99.9 (100.0)
Redundancy	13.8 (12.7)
$\langle I/\sigma(I) \rangle$	49.8 (3.7)
R_{meas}	0.027 (0.737)
Overall B factor from Wilson plot (Å^2)	14.4

Values for the outer shell are given in parentheses.

3.2. Alpha-Amylase Crystallization

3.2.1. Preliminary Crystallization by the Microbatch Method to Develop a Crystallization Strategy

To carry out the preliminary experiment, we referred to previous alpha-amylase crystallization experiments and calculated the electrostatic value of alpha-amylase according to its C-profile (MB2004-CRT700; Confocal Science Inc.). In our previous crystallization experiments of alpha-amylase, fewer and thicker crystals grew at higher PEG 4000 concentrations (data not shown). The electrostatic repulsive force between alpha-amylase molecules in its crystal was nearly cancelled in a 200 mM sodium chloride solution at pH 7.0. Therefore, to determine the upper concentration limits of PEG 4000 and sodium chloride for growing these crystals, we performed preliminary batch crystallization of alpha-amylase at 20 degrees Celsius using a limited concentration region around known crystallization conditions: 15–25% (*w/v*) PEG 4000 (162-09115; FUJIFILM Wako Pure Chemical Corporation) and 50–200 mM sodium chloride (31320-05; NACALAI TESQUE, Inc., Kyoto, Japan). The concentration of alpha-amylase from *Aspergillus oryzae* was fixed at 30 mg/mL (MB-P-AD001; Confocal Science Inc.). All solutions were dissolved in 50 mM HEPES buffer pH 7.0 (17514-15; NACALAI TESQUE, Inc.) containing 2 mM calcium chloride (06731-05; NACALAI TESQUE, Inc.). Each crystallization experiment was carried out in duplicate. After ten days, the number of single and clustered crystals was counted by visual inspection, and the number of crystals in a unit volume (1 μL) and the ratio of single crystals to all crystals were calculated (Table 5).

For all conditions exhibiting crystal growth, the number of crystals was small, which suggested that these crystallization conditions were optimal to proceed with our crystallization strategy. In 200 mM sodium chloride, single crystals were obtained with 20% (*w/v*) PEG 4000 but not at lower PEG 4000 concentrations. In 23% (*w/v*) PEG 4000, single crystals were obtained with 100 mM sodium chloride but not at lower sodium chloride concentrations. Because a few single crystals grew in low concentrations of PEG 4000 and/or sodium chloride, the concentrations were increased to 23% (*w/v*) PEG 4000 and 200 mM sodium chloride.

Table 5. Number of crystals in unit volume and the ratio of single crystals of alpha-amylase grown by microbatch crystallization in sodium chloride and PEG 4000. The table shows the number of crystals per unit volume (1 μL) (top number) and the ratio of single crystals to all crystals (bottom number) ten days after crystallization setup.

|			Sodium Chloride (mM)			
			50	100	150	200
PEG 4000 (%(*w/v*))	25		0	3	Precipitation	Precipitation
			-	0.00	-	-
	24		0	2	Precipitation	Precipitation
			-	0.50	-	-
	23		0	2	8	3
			-	1.00	0.75	0.00
	22		0	3	2	4
			-	0.67	1.00	0.00
	21		6	8	4	5
			0.67	0.38	0.75	0.60
	20		ND	7	ND	2
			ND	0.00	ND	1.00
	15		ND	0	ND	0
			ND	-	ND	-

ND: No data. The color depth of the cell corresponds to the single crystal ratio.

Two strategies were considered for crystallization with the device. One was to fix the sodium chloride concentration at 200 mM and gradually increase the concentration of PEG 4000 to 23% (*w/v*). The other was to fix the PEG 4000 concentration at 23% (*w/v*) and gradually increase the sodium chloride concentration to 200 mM. The latter strategy failed, with the formation of many crystals. This might be because the high PEG 4000 concentration caused crystallization when there were small fluctuations around this concentration. Alternatively, there might have been regions where the nucleation probability was high in the 23% (*w/v*) PEG 4000 solution when the sodium chloride concentration was lower than 50 mM [18]. Therefore, we adopted the first strategy of gradually increasing the concentration of PEG 4000 to 23% (*w/v*) while using a fixed sodium chloride concentration of 200 mM. The starting PEG 4000 concentration was 15% (*w/v*) in which no crystals were observed (Table 5).

3.2.2. Alpha-Amylase Crystallization Using the Device to Grow Large Crystals

Crystallization was performed at 20 degrees Celsius in the device following the procedure in Figure 4 and was based on the preliminary batch crystallization results. The alpha-amylase solution in the crystallization cell was 30 μL of 30 mg/mL alpha-amylase, 15% (*w/v*) PEG 4000 and 200 mM sodium chloride in 50 mM HEPES buffer pH 7.0 and 2 mM calcium chloride. Initially, 10 mL of 15% (*w/v*) PEG 4000 and 200 mM sodium chloride in 50 mM HEPES buffer pH 7.0 and 2 mM calcium chloride (Reservoir D) was filled in the reservoir container and flowed at 240 μL/min into the crystallization cell for three days to confirm that no crystallization occurred. On Day 3, 45% (*w/v*) PEG 4000 and 200 mM sodium chloride in 50 mM HEPES buffer pH 7.0 and 2 mM calcium chloride (Reservoir E) was flowed into the reservoir container at a flow rate of 0.14 μL/min to increase the PEG 4000 concentration. At the same time, the desiccator pump was activated to feed dry air at a flow rate of 0.5 mL/min to stimulate nucleation. For technical reasons, all pumps were stopped from Day 11 until Day 16. During this time interval, the concentration of PEG 4000 in the reservoir container was 21% (*w/v*). On Day 17, Reservoir E was again flowed into the reservoir container. On Day 18, three crystals, the largest of which was 0.5 mm in length, formed in the middle of the crystallization cell, and five crystals formed near the dry air probe (Figure 5a). All pumps were stopped to allow the crystals to further grow under this condition. On Day 19, five crystals had grown to a size of 1.16 mm in

length (Figure 5b). On Day 21, the crystals had grown to 1.4 mm in length and were expected to grow further under the same conditions, but many small crystals had begun to form. Therefore, Reservoir E was flowed into the reservoir container again to increase the PEG 4000 concentration in the crystallization cell to cause PEG-induced depletion attraction [18]. On Day 24, the concentration of PEG 4000 in the reservoir container reached 23% (*w/v*), and all pumps were stopped. On Day 28, the crystals were 1.4–1.5 mm in length (Figure 5c).
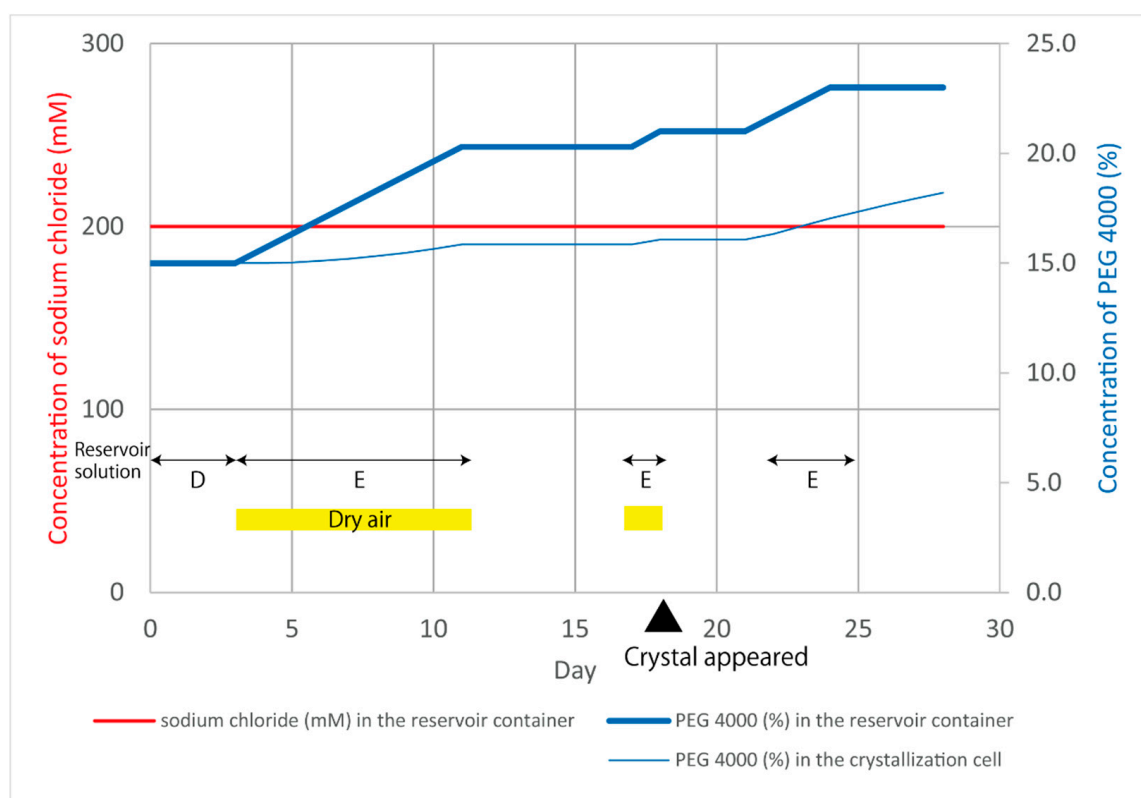
Figure 4. Controlling alpha-amylase crystallization conditions by changing the reservoir solution. The concentration of PEG 4000 in the reservoir container and the estimated concentration of PEG 4000 in the crystallization cell are shown as thick blue lines and thin blue lines, respectively. The concentration of sodium chloride (red line) was fixed during the experiment. The reservoir solution flowing to the reservoir container was changed as indicated by the black double arrows: D, 15% (*w/v*) PEG 4000 at a flow rate of 240 µL/min; E, 45% (*w/v*) PEG 4000 at a flow rate of 0.14 µL/min. All solutions were dissolved in 50 mM HEPES buffer pH 7.0 containing 200 mM sodium chloride and 2 mM calcium chloride. Dry air was supplied at a flow rate of 0.5 mL/min during the first and second flows of Reservoir E.

To verify the quality of the alpha-amylase crystals, they were subjected to X-ray diffraction at room temperature by applying a wavelength of 1.12 Å on the BL2S1 beamline at AichiSR, Japan, using an ADSC 210 detector system [20]. The crystallization cell was cut by a file to remove the mother liquor around the crystals. The end of the crystallization cell was sealed with wax (HR4-328, Hampton Research, CA, USA) to prevent solvent evaporation and then mounted to the goniometer head. The data were collected at 293 K. A total of 720 frames were collected using a crystal-to-detector distance of 127.0 mm with a 3-s exposure time and a 0.5° oscillation angle. The diffraction images of alpha-amylase were integrated using XDS23 and scaled using Aimless in the CCP4 suite [21].

The data collection and processing statistics are shown in Table 6. The maximum resolution was 1.57 Å with low mosaicity (0.11°). The resolution of the obtained alpha-amylase crystals was similar to the highest resolution of those deposited in the Protein Data Bank (PDB ID: 6XSJ). We concluded that the crystallization device and strategy were effective not only for growing large crystals but also high-quality crystals of alpha-amylase.
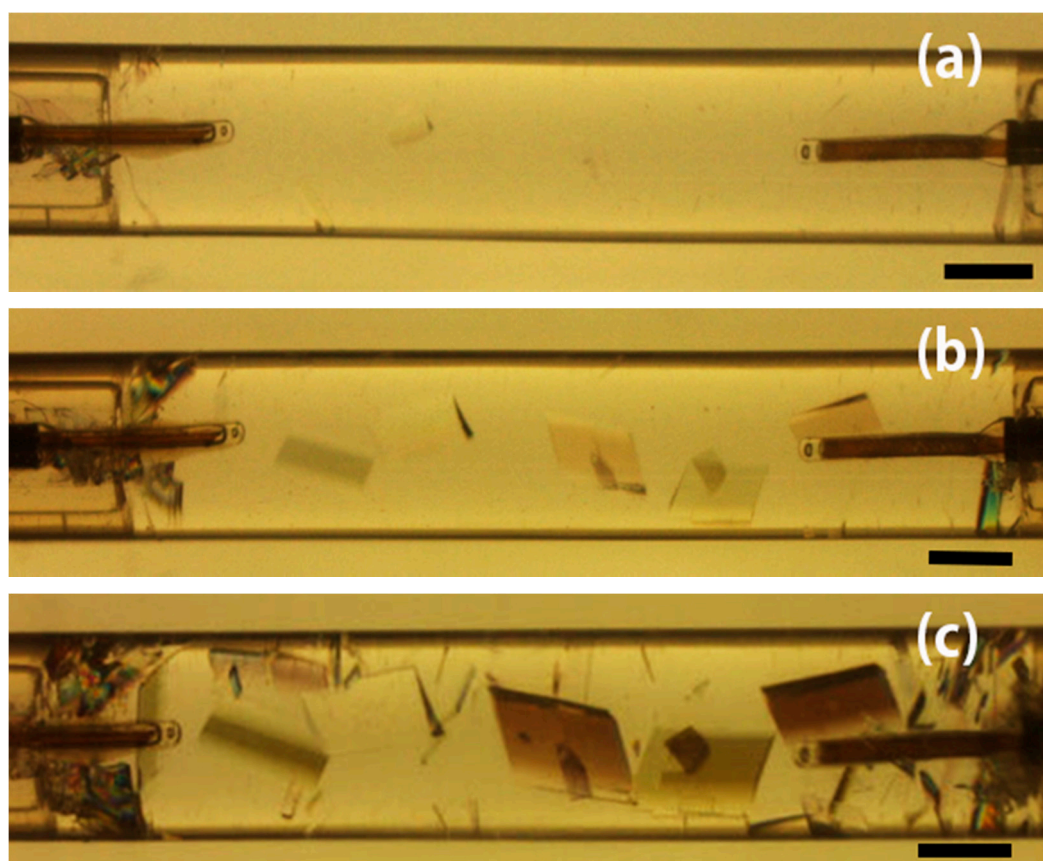
Figure 5. Alpha-amylase crystals grown in the crystallization cell. (**a**) Eighteen days after crystallization set up, three small crystals were observed in the middle of the crystallization cell. (**b**) On Day 19, five 1.16 mm crystals were observed. (**c**) On Day 28, the largest crystals were 1.4 to 1.5 mm. The scale bars correspond to 1 mm.

Table 6. Data collection and processing of alpha-amylase crystals.

Diffraction Source	BL2S1, AichiSR
Wavelength (Å)	1.12
Temperature (K)	293
Detector	ADSC 210
Crystal-detector distance (mm)	127.0
Rotation range per image (°)	0.5
Total rotation range (°)	360
Exposure time per image (s)	3
Space group	$P2_1$
a, b, c (Å)	67.1, 104.5, 76.0
α, β, γ (°)	90.0, 104.5, 90.0
Mosaicity (°)	0.11
Resolution range (Å)	43.58–1.57 (1.60–1.57)
Total No. of reflections	513,229 (25,341)
No. of unique reflections	139,941 (6942)
Completeness (%)	99.2 (99.7)
Redundancy	3.7 (3.7)
$\langle I/\sigma(I)\rangle$	12.9 (2.0)
R_{meas}	0.045 (0.597)
Overall B factor from Wilson plot (Å^2)	18.0

Values for the outer shell are given in parentheses.

4. Discussion

Here, we introduce a method for the rational growth of large, high-quality protein crystals that does not depend on luck. The developed device utilizes dialysis and is equipped with a liquid feeding mechanism. The concentration of the crystallization solution in the crystallization cell can be controlled throughout the experiment, unlike other crystallization methods. Moreover, each component of the crystallization solution can be controlled individually, resulting in the growth of low numbers of large crystals. The real-time observation system is useful for controlling the crystallization conditions while observing crystal growth. Nucleation was stimulated by supplying dry air, which led to the growth of small numbers of crystals even in a condition in which nucleation was unlikely to occur.

To maximize the performance of this device for growing large crystals, a pre-established crystallization condition is essential.

Preliminary microbatch crystallization in various concentration ranges of precipitant components was performed for lysozyme crystallization. The nucleation and crystal growth depended on the concentration of sodium chloride and PEG 4000. High-quality crystals were obtained at high concentrations of PEG 4000, and the solubility of the protein decreased as the concentrations of PEG 4000 and sodium chloride increased. For proteins where the crystallization conditions are not well defined, it is recommended to test many crystallization conditions in the preliminary crystallization experiments, as we did for lysozyme. This may take some time, but it will improve future efficiency. Because real-time crystallization in the device can be observed, the scope of the preliminary experiments can be narrowed down to some extent. For well-studied protein samples, preliminary experiments such as those performed with alpha-amylase can be adopted.

Based on the results of the preliminary experiments, we controlled the sodium chloride and PEG concentrations and (if required) the supply of dry air to the crystallization cell to stimulate nucleation. We obtained 1.8 mm lysozyme and 1.5 mm alpha-amylase crystals with good reproducibility. X-ray diffraction data sets of the lysozyme and alpha-amylase crystals were collected at room temperature and showed good diffraction—1.39 Å resolution for lysozyme and 1.57 Å for alpha-amylase, with low mosaicity. This crystallization device and strategy worked effectively to grow large, high-quality protein crystals that could be applied to neutron diffraction experiments. However, there are still some difficulties in growing a single large crystal in the crystallization cell, which would be optimal. We aim to further develop this device and strategy, such as improving the accuracy of the estimated concentrations in the crystallization cell. To increase its versatility, we will also further optimize the reservoir probe so that it can be used with other reagents such as higher molecular weight PEGs, which are commonly used as precipitants in protein crystallization. In the future, it may be possible to equip more pumps for solution supply to increase the number of controllable chemicals in the crystallization solution. Developing a protein supply system for the crystallization cell may also be preferable for growing larger crystals.

5. Patents

PCT/JP2017/046880, Tanigawa Naoki, Tanaka Hiroaki, Takahashi Sachiko, Inaka Koji, Protein crystallization method and crystallization device, Chiyoda Corp., Kanagawa, Japan and Confocal Science Inc., 27 December 2017.

Author Contributions: Conceptualization, N.T. and H.T.; methodology, N.T., S.T. and H.T.; validation, N.T., M.K., N.F., K.I., S.T., B.Y. and H.T.; formal analysis, M.K., N.F. and K.I.; investigation, S.T. and H.T.; resources, N.T. and H.T.; data curation, N.T., S.T. and H.T.; writing—original draft preparation, S.T. and H.T.; writing—review and editing, N.T., S.T., K.K., K.I. and H.T.; visualization, N.T.; supervision, H.T.; project administration, N.T. and H.T. All authors have read and agreed to the published version of the manuscript.

References

1. Helliwell, J.R. New Developments in crystallography: Exploring its technology, methods and scope in the molecular biosciences. *Biosci. Rep.* **2017**, *37*, BSR20170204. [CrossRef]
2. Blakeley, M.P.; Cianci, M.; Helliwell, J.R.; Rizkallah, P.J. Synchrotron and neutron techniques in biological crystallography. *Chem. Soc. Rev.* **2004**, *33*, 548–557. [CrossRef]
3. Niimura, N.; Podjarny, A. Experimental procedure for neutron protein crystallography. In *Neutron Protein Crystallography*; Oxford University Press: Oxford, UK, 2011.
4. Meilleur, F.; Coates, L.; Cuneo, M.J.; Kovalevsky, A.; Myles, D.A.A. The neutron macromolecular crystallography instruments at Oak Ridge National Laboratory: Advances, challenges, and opportunities. *Crystals* **2018**, *8*, 388. [CrossRef]
5. Tanaka, I.; Chatake, T.; Fujiwara, S.; Hosoya, T.; Kusaka, K.; Niimura, N.; Yamada, T.; Yano, N. Current status and near future plan of neutron protein crystallography at J-PARC. *Methods Enzymol.* **2020**, *634*, 101–123. [PubMed]
6. Galkin, O.; Vekilov, P.G. Nucleation of protein crystals: Critical nuclei, phase behavior, and control pathways. *J. Cryst. Growth* **2001**, *232*, 63–76. [CrossRef]
7. Ng, J.D.; Baird, J.K.; Coates, L.; García-Ruiz, J.M.; Hodge, T.A.; Huang, S. Large-volume protein crystal growth for neutron macromolecular crystallography. *Acta Cryst.* **2015**, *F71*, 358–370. [CrossRef] [PubMed]
8. Ostwald, W. Studien über die Bildung und Umwandlung fester Körper. *Z. Phys. Chem.* **1897**, *22*, 289–330. [CrossRef]
9. Nakamura, H.; Takahashi, S.; Inaka, K.; Tanaka, H. Semi-empirical model to estimate ideal conditions for the growth of large protein crystals. *Acta Cryst.* **2020**, *D76*, 1174–1183.
10. Budayova-Spano, M.; Dauvergne, F.; Audiffren, M.; Bactivelane, T.; Cusack, S. A methodology and an instrument for the temperature-controlled optimization of crystal growth. *Acta Cryst.* **2007**, *D63*, 339–347. [CrossRef]
11. Junius, N.; Vahdatahar, E.; Oksanen, E.; Ferrer, J.-L.; Budayova-Spano, M. Optimization of crystallization of biological macromolecules using dialysis combined with temperature control. *J. Appl. Cryst.* **2020**, *53*, 686–698. [CrossRef]
12. Yamaguchi, S.; Sunagawa, N.; Matsuyama, K.; Tachioka, M.; Hirota, E.; Takahashi, S.; Igarashi, K. Preparation of large-volume crystal of cellulase under microgravity to investigate the mechanism of thermal stabilization. *Int. J. Microgravity Sci. Appl.* **2021**, *38*, 380103.
13. Volmer, M.; Weber, A. Keimbildung in übersättigten Gebilden. *Z. Phys. Chem.* **1926**, *119*, 277. [CrossRef]
14. Turnbull, D. Kinetics of heterogeneous nucleation. *J. Chem. Phys.* **1950**, *18*, 198. [CrossRef]
15. Yoshizaki, I.; Nakamura, H.; Fukuyama, S.; Komatsu, H.; Yoda, S. Estimation of crystallization boundary of a model protein as a function of solute concentration and experiment time. *J. Microgravity Sci. Appl.* **2002**, *19*, 30–33.
16. Allan, D.R.; Collins, S.P.; Evans, G.; Hall, D.; McAuley, K.; Owen, R.L.; Sorensen, T.; Tang, C.C.; von Delft, F.; Wagner, A.; et al. Status of the crystallography beamlines at Diamond Light Source. *Eur. Phys. J. Plus* **2015**, *130*, 56. [CrossRef]
17. Vonrhein, C.; Flensburg, C.; Keller, P.; Sharff, A.; Smart, O.; Paciorek, W.; Womack, T.; Bricogne, G. Data processing and analysis with the autoPROC toolbox. *Acta Cryst.* **2011**, *D67*, 293–302.
18. Tardieu, A.; Bonneté, F.; Finet, S.; Vivarés, D. Understanding salt or PEG induced attractive interactions to crystallize biological macromolecules. *Acta Cryst.* **2002**, *D58*, 1549–1553. [CrossRef]
19. Bradford, M. A rapid and sensitive method for the quantitation of microgram quantities of protein utilizing the principle of protein-dye binding. *Anal. Biochem.* **1976**, *72*, 248–254. [CrossRef]
20. Watanabe, N.; Nagae, T.; Yamada, Y.; Tomita, A.; Matsugaki, N.; Tabuchi, M. Protein crystallography beamline BL2S1 at the Aichi synchrotron. *J. Synchrotron Rad.* **2017**, *24*, 338–343. [CrossRef] [PubMed]
21. Battye, T.G.; Kontogiannis, L.; Johnson, O.; Powell, H.R.; Leslie, A.G. iMOSFLM: A new graphical interface for diffraction-image processing with MOSFLM. *Acta Cryst.* **2011**, *D67*, 271–281. [CrossRef]
22. Evans, P.R.; Murshudov, G.N. How good are my data and what is the resolution? *Acta Cryst.* **2013**, *D69*, 1204–1214. [CrossRef] [PubMed]